Functional and structural studies of the Abruptex region of the Notch receptor

A thesis submitted for the degree of Doctor of Philosophy by Zhi Han Bo,

Department of Biochemistry, St Cross College, Michaelmas term 2024

Appendix

Table of Contents

Appendix A – PCR recipe and primers 2

Appendix B – *E. coli* transformation 8

Appendix C – Protein purification buffers 10

Appendix D – Protein analysis buffers 12

Appendix E – Activation assays 14

Appendix F – Cis-inhibition assays 17

Appendix G – Assays in the presence of Lfng 21

Appendix H – SAXS 27

Appendix I – Discussion 30

Appendix A – PCR recipe and primers

Table A.1. Recipe for KOD Polymerase PCR reaction.

Component	Volume per 50 µl PCR reaction (µl)
Milli-Q (MQ) water	Make reaction volume up to 50 µl
10x KOD Buffer	5
25 mM MgSO4	3
2 mM dNTPs	5
10 µM Forward Primer	1.5
10 µM Forward Primer	1.5
KOD Polymerase (1U/µl)	1

Table A.2. PCR thermocycling conditions.

Step	Target size			
	<500 bp	500– 1000 bp	1000 – 3000 bp	>3000 bp
1. Polymerase activation	95 °C for 2 mins			
2. Denaturation	95 °C for 20s			
3. Annealing	55 °C			
4. Extension	70 °C for 10 s/kb	70 °C for 15 s/kb	70 °C for 20 s/kb	70 °C for 15 s/kb
Repeat steps 2-4	30 cycles			
5. Final extension	70 °C for 10 mins			
6. End	4 °C forever			

Table A.3. Primers used in this project.

Usage	Forward (F) /Reverse (R)	Name	Primer sequence 5' - 3'
mN1 overlap extension mutagenesis (backbone primers)	F	For_end_Sbf1	ACACCTGCAGGCAAGATGTTAATGAGTGCAGCCAGAACCC
	R	Rev_end_BamH1	GAAGGATCCCAGGCATAGGCAGGTGGGACTACGTGGG
	F	For_end_Sbf1_1	ACACCTGCAGGCAAGATGTTAATGAG
	R	Rev_end_BamH1_1	GAAGGATCCCAGGCATAGGCAGG
	F	For_end_ClaI_1	AATGAGTGTGTGAAAAGCCCATGTCGCC

mN1 mutagenesis (mN1 L468A)	F	mouseN1_L468A_F	CAGAATGATGCCACTTGCGC CGACCAGATTGGGGAGTTC
	R	mouseN1_L468A_R	GAACTCCCCAATCTGGTCGG CGCAAGTGGCATCATTCTG
mN1 mutagenesis (mN1 Q462R)	F	mN1_Q462R_F_1	TGCATCTCCAACCCATGTCGC AATGATGCCACTTGCCTG
	R	mN1_Q462R_R_1	CAGGCAAGTGGCATCATTGC GACATGGGTTGGAGATGCA
mN1 mutagenesis (mN1 G632R)	F	mouseN1_G632R_ F	TGCCTCAAGCGAACCACAGG GCCCAAC
	R	mouseN1_G632R_ R	CTGTGGTTCGCTTGAGGCATA AGCAG
mN1 mutagenesis (mN1 G635D)	F	mouseN1_G635D_ F	GAACCACAGATCCCAACTGT GAGATCAAC
	R	mouseN1_G635D_ R	ACAGTTGGGATCTGTGGTTC CCTTGAGGC
mN1 mutagenesis (mN1 D909V)	F	mouseN1_D909V_F	AACTGTGAGAGTGACATCGT GGACTGCCGCCCCAACCCG
	R	mouseN1_D909V_ R	CGGGTTGGGGCGGCAGTCC ACGATGTCACTCTCACAGTT
mN1 mutagenesis (mN1 C933S)	F	mouseN1_C933S_F	CTTCTGCGACAGTCTGCCCG GCTTCCAGGGTG
	R	mouseN1_C933S_ R	CCGGGCAGACTGTCGCAGAA GGCTGTGTTGATG
mN1 mutagenesis (mN1 N947I)	F	mouseN1_N947I_F	TTCTGTGAGGAGGACATCATT GAATGTGCCAGCAATCCC
	R	mouseN1_N947I_R	GGGATTGCTGGCACATTCAAT GATGTCCTCCTCACAGAA
mN1 mutagenesis (mN1 C960Y)	F	mouseN1_C960Y_F _2	CCAAAATGGTGCCAATTATAC TGACTGTGTGGACAGCTACA C
	R	mouseN1_C960Y_ R_2	GCTGTCCACACAGTCAGTATA ATTGGCACCATTTTGGCAGG G

mN1 mutagenesis (mN1 S990N)	F	mouseN1_S990N_F_2	CACCTGACTGTACTGAGAATTCCTGCTTCAATGGTGGTACCTG
	R	mouseN1_S990N_R_2	CCACCATTGAAGCAGGAATTCTCAGTACAGTCAGGTGTGTTG
mN1 mutagenesis (mN1 Q1049I)	F	mouseN1_Q1049I_F_2	GTGTACCTGCCCAATAGGCTACACTGGTCTCAACTGC
	R	mouseN1_Q1049I_R_2	GTTGAGACCAGTGTAGCCTATTGGGCAGGTACACTTATAAGTACC
mN1 mutagenesis (mN1 H1129Y)	F	mN1_H1129Y_F_1	GTGGATGAGGGAGATAAATATTACTGCCACTGCCAGGCA
	R	mN1_H1129Y_R_1	TGCCTGGCAGTGGCAGTAATATTTATCTCCCTCATCCAC
mN1 mutagenesis (mN1 G1136A)	F	mN1_G1136A_F_1	TACTGCCACTGCCAGGCAGCCTACACGGGCAGCTACTGT
	R	mN1_G1136A_R_1	ACAGTAGCTGCCCGTGTAGGCTGCCTGGCAGTGGCAGTA
mN1 mutagenesis (mN1 R1279H)	F	mouseN1_R1279H_F	GTGACCCACATGGCACCCAGAACTGTGTGCAG
	R	mouseN1_R1279H_R	GTTCTGGGTGCCATGTGGGTCACAGGGGTTGGAGAGACATTC
mN1 mutagenesis (mN1 N1289S)	F	mouseN1_N1289S_F	GTGTGCAGCGTGTTAGTGACTTCCACTGCGAGTGCCG
	R	mouseN1_N1289S_R	CAGTGGAAGTCACTAACACGCTGCACACAGTTCTGGGTG
mN1 mutagenesis (mN1 G1301R)	F	mN1_G1301R_F	GCCACACTAGACGCCGCTGTGAGTCAGTCATC
	R	mN1_G1301R_R	CACAGCGGCGTCTAGTGTGGCCAGCCCGGCAC
mN1 mutagenesis (mN1 E1305K)	F	mN1_E1305K_F	CGCCGCTGTGAATCAGTCATCAATGGCTGCAGGGG
	R	mN1_E1305K_R	CATTGATGACTGATTCACAGC

			GGCGTCCAGTGTG
mN1 genomic DNA amplification and sequencing (LBR)	F	mN1_LBR_For	CATTGATGACTGTGCCAGTGC
	R	mN1_LBR_Rev	CCGTTCTTGCATGGTGTG
mN1 genomic DNA amplification and sequencing (EGF16)	F	mN1_EGF16_F	TGTCTGCACAATGGCCACTG
	R	mN1_EGF16_R	CAATTAGGGCCACTGAAGCC
mN1 genomic DNA amplification and sequencing (Ax N terminus)	F	mN1_Ax_For	GTGCCCCTGGGTGGAGTGGAAC
	R	mN1_Ax_Rev	ATCCACACAGGTACCACCATTGAAGCAG
mN1 genomic DNA amplification and sequencing (Ax C terminus)	F	mN1_EGF26-29_F	TTCCAGGGTGCCTTCTGTGAG
	R	mN1_EGF26-29_R	CATTGATCTCACAGTGTACACCCTG
mN1 genomic DNA amplification and sequencing (EGF33)	F	mN1_SeqFor_8	TGACCAACTCCTACAAGTGTTCCT
	R	Rev_end_BamH1_1	GAAGGATCCCAGGCATAGGCAGG
mN1 sequencing	R	mN1_SeqRev_1	ACCCCCATTCTTGCAGTTGTTTCC
	F	mN1_SeqFor_1	GGAAACAACTGCAAGAATGGGGGT
	F	mN1_SeqFor_2	TTTCCAGGGTGCCACTTGCCACGA
	F	mN1_SeqFor_3	GAAATCAACACGGATGAGTG

			CGCC
	F	mN1_SeqFor_4	AGATCAACCTGGATGACTGC GCCA
	F	mN1_SeqFor_5	GGCCCTAATTGCCAGACCAA CATC
	F	mN1_SeqFor_6	GGAGGACATCAATGAATGTG CCAG
	F	mN1_SeqFor_7	GCACAGAAGCGAGGCATTGA CGTC
	F	mN1_SeqFor_8	TGACCAACTCCTACAAGTGTT CCT
hDLL4 sequencing		RDLL4Q2	ACAGTCGCTGACGTGGAGTT CA
pUC19 plasmid sequencing	F	pUC19_For	GCTTCCGGCTCGTATGTTGTG TGGAATTGTGAGC
	R	pUC19_Rev	GATCGGTGCGGGCCTCTTCG CTATTACGC
pHLsec plasmid sequencing	F	pHLsec_Fwd	GGCGGCTCTAGAGCCTCTGC
	R	pHLsec_Rev	CCGGGAGATCATGAGGGTGT C
pcDNA3.1(+) plasmid sequencing	F	T7 promoter (F) (Source Bioscience)	TAATACGACTCACTATAGGG
	R	BGH Reverse (Source Bioscience)	TAGAAGGCACAGTCGAGG
	F	pcDNA3.1_Fwd	GCGGTTTTGGCAGTACATCAA T
	R	pcDNA3.1_Rev	TAGAGCCCCAGCTGGTTCTTT
pOG44 plasmid sequencing	F	CMVF_pCDNA3 (Source Bioscience)	CAACGGGACTTTCCAAAATG
	R	T3 (Source Bioscience)	ATTAACCCTCACTAAAG
pEXS2-2 plasmid sequencing	F	pEXS2_2_Fwd	GGTAAAAGTTTTGAACGCG
	R	pEXS2_2_Rev	CGCGCTTGAAAGGAGTGTG
pAPtag2 plasmid	F	pAPtag2_Seq_1	GAAGATGATGAGGTTCTTGG C

sequencing			
RT-PCR (mN1)	F	mN1_RT_For_2	CAACAACGAGTGTGAGTCCAACCC
	R	mN1_RT_Rev_1	GGTTTGACCTTGCCAGCCTGTG
RT-PCR (hJAG1)	F	hJ1_RT_F_ZB	GTCGGGATTTGGTTAATGGTTATCGC
	R	hJ1_RT_R_1_ZB	TAGTCACTGGCACGGTTGTAGCAC
RT-PCR (hDLL4)	F	hDLL4_RT_F	CTGCGAGAAGAAAGTGGACAGG
	R	hDLL4_RT_R	ACAGTCGCTGACGTGGAGTTCA
RT-PCR (mLfng)	F	mLfng_RT_F_1_ZB	AGCGAGCACAAAGTGAGACCTG
	R	mLfng_RT_R_ZB	GATGGGTCAGCTTCCACAGAG
RT-PCR (mRfng)	F	mRfng_RT_F_ZB	TGCTGCTGCGTACCTGGATCTC
	R	mRfng_RT_R_ZB	CAGGTAGATGTCCTGGTTGGAAGAG
RT-PCR (GAPDH)	F	GAPDH_M_For_2	GATTTGGTCGTATTGGGCGC
	R	GAPDH_M_Rev_1	CGCCCCACTTGATTTTGGAG
Cloning of full-length hDLL4 WT	F	BamHI_hDLL4_Fwd_1	ATGGATCCGCCATGGCGGCAGCGTCCC
	R	hDLL4_NotI_Rev_1	ATGCGGCCGCTTATACCTCCGTGGCAATGACACATTC

Appendix B – *E. coli* transformation

Table B.1. NEB® 5-alpha Competent *E. coli* transformation protocol.

Step	Procedure
1	Thaw frozen *E. coli* stock on ice for 10 minutes.
2	Add 1 µl purified plasmid stock or 2.5 µl ligation mixture into 50 µl Competent *E. coli.* Mix gently by flicking the tube.
3	Incubate *E. coli* on ice for 30 minutes.
4	Heat shock *E. coli* at 42 °C for exactly 30 seconds.
5	Incubate *E. coli* on ice for 5 minutes.
6	Mix 50 µl *E. coli* with 950 µl room temperature SOC outgrowth medium (NEB).
7	Incubate *E. coli* at 37 °C, 300 rpm for 1 hour.
8	Spread 30 µl (for purified plasmid) or 200 µl (for ligation mixture) of *E. coli* outgrowth culture onto an agar plate with suitable selective antibiotics.
9	Incubate the agar plate overnight at 37 °C.
10	Select successfully transformed colonies for expansion.

Table B.2. MC1061 P3 Competent *E. coli* transformation protocol.

Step	Procedure
1	Thaw frozen *E. coli* stock on ice for 10 minutes.
2	Add 5 µl purified plasmid stock into 100 µl Competent *E. coli*. Mix gently by flicking the tube.
3	Incubate *E. coli* on ice for 30 minutes.
4	Heat shock *E. coli* at 42 °C for exactly 30 seconds.
5	Incubate *E. coli* on ice for 2 minutes.
6	Mix 100 µl *E. coli* with 900 µl room temperature SOC outgrowth medium (NEB).
7	Incubate *E. coli* at 37 °C, 300 rpm for 1 hour.
8	Spread 100 µl of *E. coli* outgrowth culture onto an agar plate with suitable selective antibiotics.
9	Incubate the agar plate overnight at 37 °C.
10	Select successfully transformed colonies for expansion.

Table B.3. Selection conditions for plasmids.

Selection condition	Plasmid
100 mg/l ampicillin	pUC19, pcDNA5/FRT, pOG44, pcDNA3.1(+), pHLsec
50 mg/l kanamycin	pEXS2.2
25 mg/l ampicillin, 10 mg/l tetracycline	pAPtag2

Appendix C – Protein purification buffers

Table C.1. Recipe for Tris gel filtration buffer, pH 9.0, 0.22 µm filtered, stored at 4 °C.

Component	Concentration (mM)
Tris-HCl	50
NaCl	200

Table C.2. Recipe for MES gel filtration buffer, pH 6.5, 0.22 µm filtered, stored at 4 °C.

Component	Concentration (mM)
MES	20
NaCl	200

Table C.3. Recipe for IMAC wash buffer for HEK293T, pH 9.0, 0.22 µm filtered, stored at 4 °C.

Component	Concentration (mM)
Tris-HCl	50
NaCl	200
Imidazole	10

Table C.4. Recipe for IMAC wash buffer for HEK293F pH 6.5, 0.22 µm filtered, stored at 4 °C.

Component	Concentration (mM)
MES	20
NaCl	200
Imidazole	50

Table C.5. Recipe for IMAC wash buffer for S2, pH 9.0, 0.22 µm filtered, stored at 4 °C.

Component	Concentration (mM)
Tris-HCl	50
NaCl	200
$CaCl_2$	5
Imidazole	2.5

Table C.6. Recipe for IMAC elution buffer for HEK293T, pH 9.0, 0.22 µm filtered, stored at 4 °C.

Component	Concentration (mM)
Tris-HCl	50
NaCl	200
Imidazole	300

Table C.7. Recipe for IMAC elution buffer for HEK293F, pH 6.5, 0.22 µm filtered, stored at 4 °C.

Component	Concentration (mM)
MES	20
NaCl	200
Imidazole	300

Table C.8. Recipe for IMAC elution buffer for S2, pH 9.0, 0.22 µm filtered, stored at 4 °C.

Component	Concentration (mM)
Tris-HCl	50
NaCl	200
$CaCl_2$	5
Imidazole	250

Table C.9. Recipe for SEC gel filtration buffer for HEK293T and HEK293F, pH 7.5, 0.22 µm filtered.

Component	Concentration (mM)
Tris-HCl	50
NaCl	200

Table C.10. Recipe for SEC gel filtration buffer for S2, pH 7.5, 0.22 µm filtered

Component	Concentration (mM)
Tris-HCl	10
NaCl	200
$CaCl_2$	5

.

Appendix D – Protein analysis buffers

Table D.1. Recipe for SDS-PAGE resolving gel, pH 8.8.

Component	Concentration
Acrylamide:bis-acrylamide, 19:1	10 – 16% W/V
SDS	0.1% W/V
Tris-HCl	0.38 M
Ammonium persulfate	0.15% W/V
N,N,N′,N′-Tetramethylethylenediamine (TEMED)	0.2% V/V

Table D.2. Recipe for SDS-PAGE stacking gel, pH 6.8.

Component	Concentration
Acrylamide:bis-acrylamide, 19:1	4% W/V
SDS	0.1% W/V
Tris-HCl	0.25 M
Ammonium persulfate	0.2% W/V
N,N,N′,N′-Tetramethylethylenediamine (TEMED)	0.2% V/V

Table D.3. Recipe for SDS-PAGE loading dye, pH 6.8.

Component	Concentration
Glycerol	10% V/V
Tris-HCl	50 mM
SDS	3% W/V
Bromophenol blue	0.2% W/V

Table D.4. Recipe for SDS-PAGE running buffer, pH 8.3.

Component	Concentration
SDS	0.1% W/V
Tris-HCl	30 mM
Glycine	250 mM

Table D.5. Recipe for western blot blotting buffer.

Component	Concentration
Glycine	190 mM
Tris-HCl	25 mM
Methanol	20% V/V
SDS	1% W/V

Table D.6. Recipe for PBST.

Component	Concentration
PBS	1x
Triton X-100	0.1% V/V

Appendix E – Activation assays

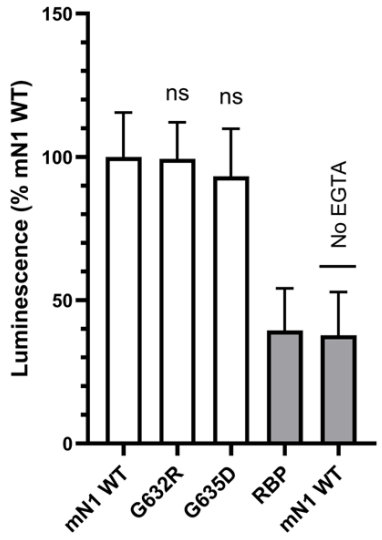

Figure E.1. Cell surface N1 level quantification for mN1 EGF16 variants.

Ligand-independent activation assay was performed for mN1 EGF16 variants. Graph shows the combined results of four independent plates, each with five repeat wells. Signal in each case is shown relative to the mN1 WT incubated with EGTA. Data presented as mean ± SD. Statistical significance compared to mN1 WT was determined by ordinary one-way analysis of variance (ANOVA) and Dunnett's post hoc test (ns = not significant).

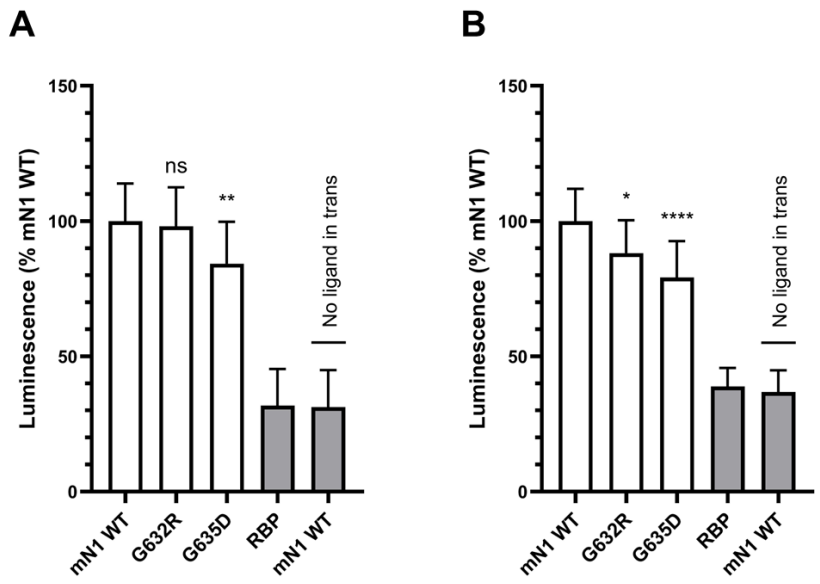

Figure E.2. Trans-activation of mN1 EGF16 variants by plate-coated protein.

Activation assay for mN1 EGF16 variants grown with plated-coated (A) hJAG1 or (B) hDLL4 NE3 protein or no coated protein (indicated by “No ligand in trans”). Graph shows the combined results of four independent plates, each with five repeat wells. Signal in each case is shown relative to the mN1 WT. Data presented as mean ± SD. Statistical significance compared to mN1 WT was determined by ordinary one-way ANOVA and Dunnett’s post hoc test (hJAG1) or Kruskal-Wallis test and Dunn’s post hoc test (hDLL4) (ns = not significant, * = $P < 0.05$, ** = $P < 0.01$, **** = $P < 0.0001$).

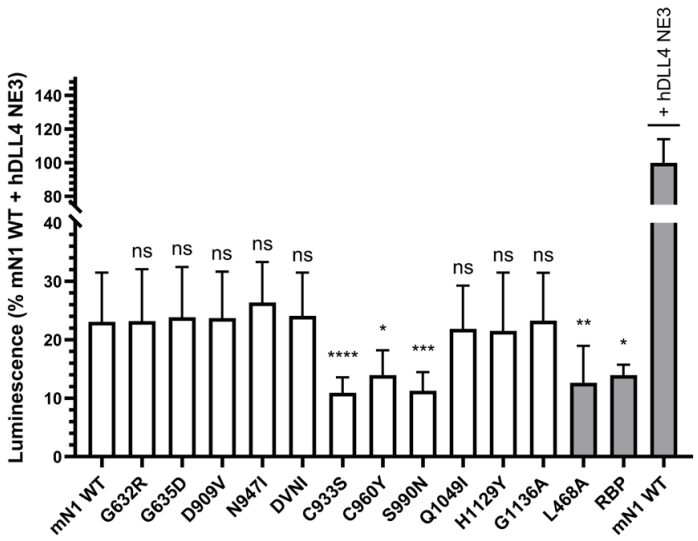

Cell line	Luminescence (% mN1 WT + hDLL4 NE3)	Statistical significance
mN1 WT + hDLL4 NE3	100 ± 13.99	
mN1 WT	23.06 ± 8.448	
G632R	23.22 ± 8.845	ns
G635D	23.86 ± 8.591	ns
D909V	23.7 ± 7.955	ns
N947I	26.39 ± 6.928	ns
DVNI	24.08 ± 7.413	ns
C933S	10.95 ± 2.622	****
C960Y	13.97 ± 4.221	*
S990N	11.29 ± 3.19	***
Q1049I	21.86 ± 7.409	ns
H1129Y	21.54 ± 9.956	ns
G1136A	23.27 ± 8.183	ns
L468A	12.67 ± 6.305	**

Figure E.3. Auto-activation levels of mN1 variants.

Activation assays for mN1 Ax variants grown without trans-ligand. Graph (left panel) and table (right panel) show the combined results of four independent plates, each with five repeat wells. Signal in each case is shown relative to the mN1 WT grown with plate-coated trans-ligand hDLL4 NE-Fc-His (indicated as + hDLL4 NE3). Data presented as mean ± SD. Statistical significance compared to mN1 WT grown without trans-ligand was determined by Kruskal-Wallis test and Dunn's post hoc test (ns = not significant, * = P < 0.05, ** = P < 0.01, *** = P < 0.001, **** = P < 0.0001).

Appendix F – Cis-inhibition assays

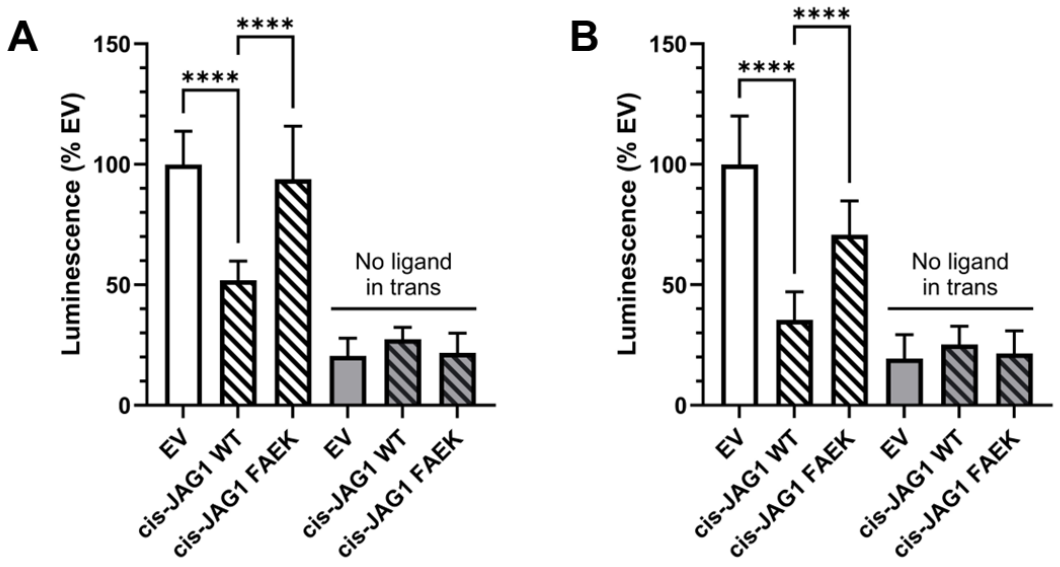

Figure F.1. Trans-activation of mN1 WT cells expressing cis-JAG1 by plate-coated protein.

Cis-inhibition assays by cis-JAG1 WT and FAEK for mN1 WT cells grown with plate-coated (A) hJAG1 NE3 or (B) hDLL4 NE3 protein or without protein (indicated by “No ligand in trans”). Graph shows the combined results of four independent plates, each with five repeat wells. Signal in each case is shown relative to cells transfected with EV. Data presented as mean ± SD. Statistical significance was determined by Welch’s ANOVA and Dunnett’s post hoc test (**** = $P < 0.0001$).

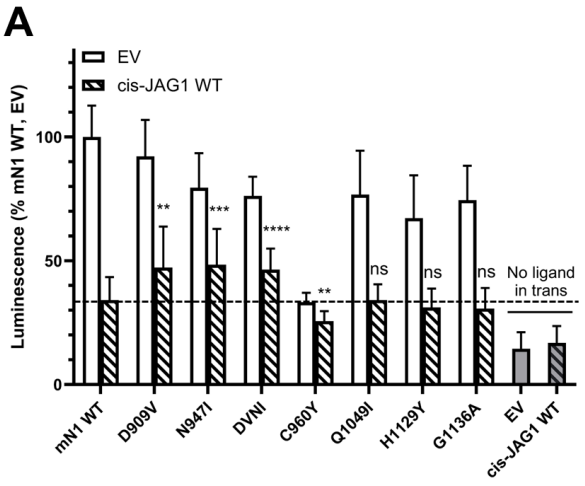

Cell line	Luminescence (% mN1 WT, EV)		Statistical significance (cis-JAG1 WT)
	EV	cis-JAG1 WT	
mN1 WT	100 ± 12.65	34.14 ± 9.263	
D909V	92.19 ± 14.71	47.31 ± 16.45	**
N947I	79.49 ± 13.92	48.4 ± 14.44	***
DVNI	76.22 ± 7.736	46.41 ± 8.517	****
C960Y	33.28 ± 3.758	25.59 ± 4.039	**
Q1049I	76.71 ± 17.72	34.13 ± 6.332	ns
H1129Y	67.21 ± 17.3	31.12 ± 7.626	ns
G1136A	74.51 ± 13.88	30.7 ± 8.292	ns

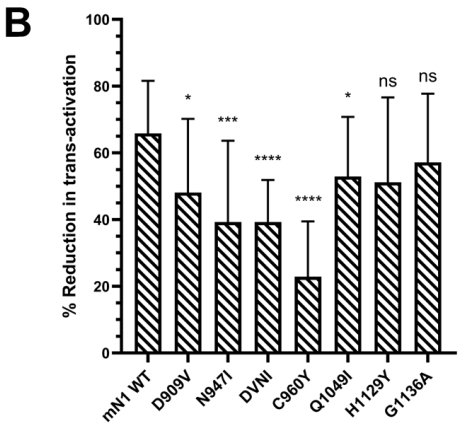

Cell line	% Reduction in trans-activation	Statistical significance
mN1 WT	65.86 ± 15.71	
D909V	48.10 ± 22.09	*
N947I	39.25 ± 24.36	***
DVNI	39.24 ± 12.64	****
C960Y	22.89 ± 16.59	****
Q1049I	52.92 ± 17.84	*
H1129Y	51.16 ± 25.45	ns
G1136A	57.16 ± 20.57	ns

Figure F.2. Trans-activation of mN1 Ax variant cells transfected with cis-JAG1 by plate-coated hJAG1 NE3 protein.

(A) Cis-inhibition assay by cis-JAG1 WT for mN1 WT and Ax variant cells grown with plate-coated hJAG1 NE3 protein or without protein (indicated by "No ligand in trans"). Signal in each case is shown relative to mN1 WT cells transfected with EV. (B) % reduction in trans-activation caused by cis-JAG1 was calculated by *(Luminescence with EV – Luminescence with cis-ligand)/Luminescence with EV x 100*. Graph (left panel) and table (right panel) show the combined results of four independent plates, each with five repeat wells. Data presented as mean ± SD. Statistical significance compared to mN1 WT transfected with cis-JAG1 was determined in (A) by Kruskal-Wallis test and Dunn's post hoc test and in (B) by Welch's ANOVA and Dunnett's post hoc test (ns = not significant, * = $P < 0.05$, ** = $P < 0.01$, *** = $P < 0.001$, **** = $P < 0.0001$).

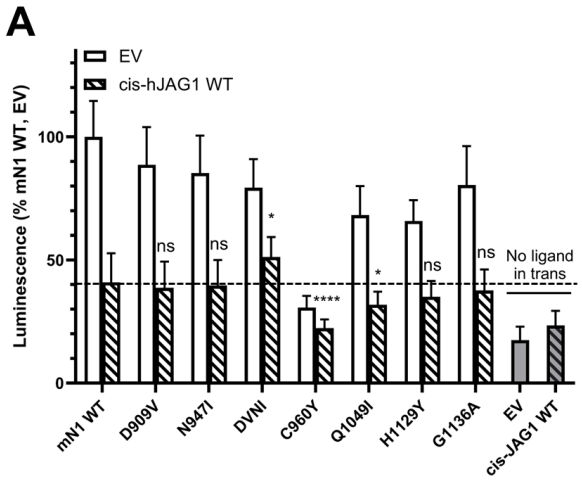

Cell line	Luminescence (% mN1 WT, EV)		Statistical significance (cis-JAG1 WT)
	EV	cis-JAG1 WT	
mN1 WT	100 ± 14.62	40.94 ± 11.78	
D909V	88.65 ± 15.32	38.7 ± 10.64	ns
N947I	85.3 ± 15.25	39.62 ± 10.35	ns
DVNI	79.37 ± 11.55	51.24 ± 8.055	*
C960Y	30.69 ± 4.736	22.35 ± 3.491	****
Q1049I	68.22 ± 11.79	31.83 ± 5.323	*
H1129Y	65.83 ± 8.451	35.04 ± 6.413	ns
G1136A	80.4 ± 15.86	37.64 ± 8.454	ns

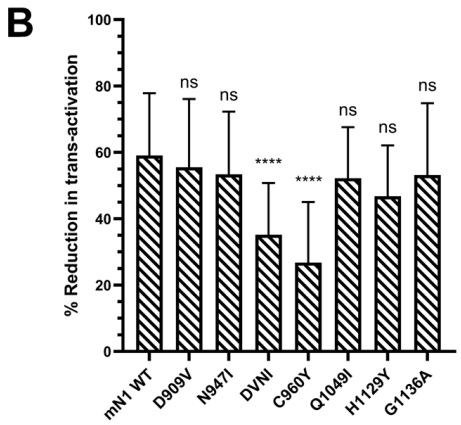

Cell line	% Reduction in trans-activation	Statistical significance
mN1 WT	59.06 ± 18.78	
D909V	55.51 ± 20.56	ns
N947I	53.39 ± 18.86	ns
DVNI	35.18 ± 15.58	****
C960Y	26.79 ± 18.24	****
Q1049I	52.22 ± 15.38	ns
H1129Y	46.75 ± 15.33	ns
G1136A	53.21 ± 21.58	ns

Figure F.3. Trans-activation of mN1 Ax variant cells transfected with cis-JAG1 by plate-coated hDLL4 NE3 protein.

(A) Cis-inhibition assay by cis-JAG1 WT for mN1 WT and Ax variant cells grown with plate-coated hDLL4 NE3 protein or without protein (indicated by "No ligand in trans"). Signal in each case is shown relative to mN1 WT cells transfected with EV. (B) % reduction in trans-activation caused by cis-JAG1 was calculated by *(Luminescence with EV – Luminescence with cis-ligand)/Luminescence with EV x 100*. Graph (left panel) and table (right panel) show the combined results of four independent plates, each with five repeat wells. Data presented as mean ± SD. Statistical significance compared to mN1 WT transfected with cis-JAG1 was determined in (A) by Kruskal-Wallis test and Dunn's post hoc test and in (B) by ordinary one-way ANOVA and Dunnett's post hoc test (ns = not significant, * = $P < 0.05$, **** = $P < 0.0001$).

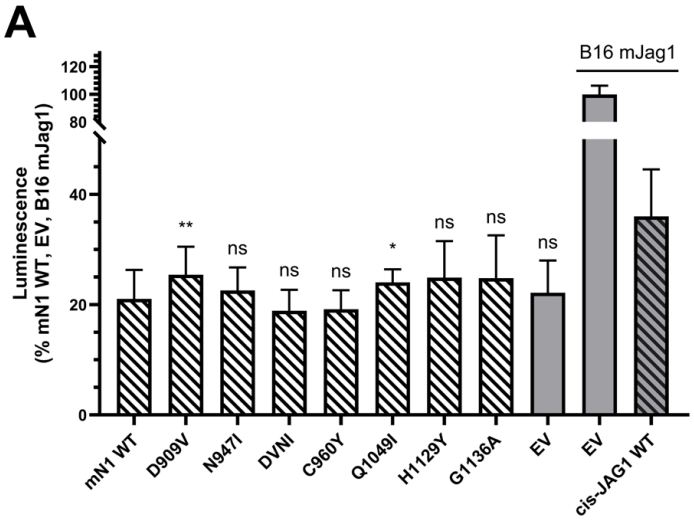

Cell line	Luminescence (% mN1 WT, EV, B16 mJag1)	Statistical significance
mN1 WT, EV, B16 mJag1	100 ± 6.265	
mN1 WT	21.07 ± 5.252	
D909V	25.43 ± 5.072	**
N947I	22.57 ± 4.197	ns
DVNI	18.88 ± 3.8	ns
C960Y	19.19 ± 3.444	ns
Q1049I	24.04 ± 2.36	*
H1129Y	24.9 ± 6.614	ns
G1136A	24.8 ± 7.764	ns
mN1 WT, EV	22.17 ± 5.851	ns

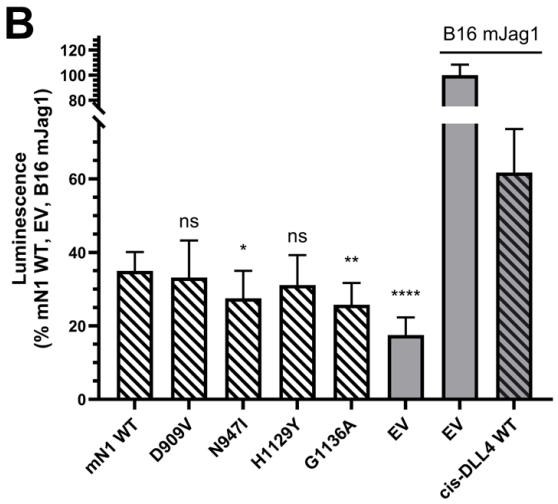

Cell line	Luminescence (% mN1 WT, EV, B16 mJag1)	Statistical significance
mN1 WT, EV, B16 mJag1	100 ± 8.306	
mN1 WT	34.97 ± 5.085	
D909V	33.12 ± 10.11	ns
N947I	27.54 ± 7.454	*
H1129Y	31.13 ± 8.141	ns
G1136A	25.73 ± 5.965	**
mN1 WT, EV	17.51 ± 4.792	****

Figure F.4. Auto-activation levels of mN1 Ax variant cells transfected with cis-JAG1/DLL4.

Activation assays for mN1 Ax variants transfected with (A) cis-JAG1 WT or (B) cis-DLL4 WT grown with B16 WT control cells. Graph (left panel) and table (right panel) show the combined results of four independent plates, each with five repeat wells. Signal in each case is shown relative to the mN1 WT cells transfected with EV grown with mJag1-expressing B16 cells (indicated by B16 mJag1). Data presented as mean ± SD. Statistical significance compared to mN1 WT transfected with cis-JAG1/DLL4 grown without trans-ligand was determined by Kruskal-Wallis test and Dunn's post hoc test (ns = not significant, * = $P < 0.05$, ** = $P < 0.01$, **** = $P < 0.0001$).

Appendix G – Assays in the presence of Lfng

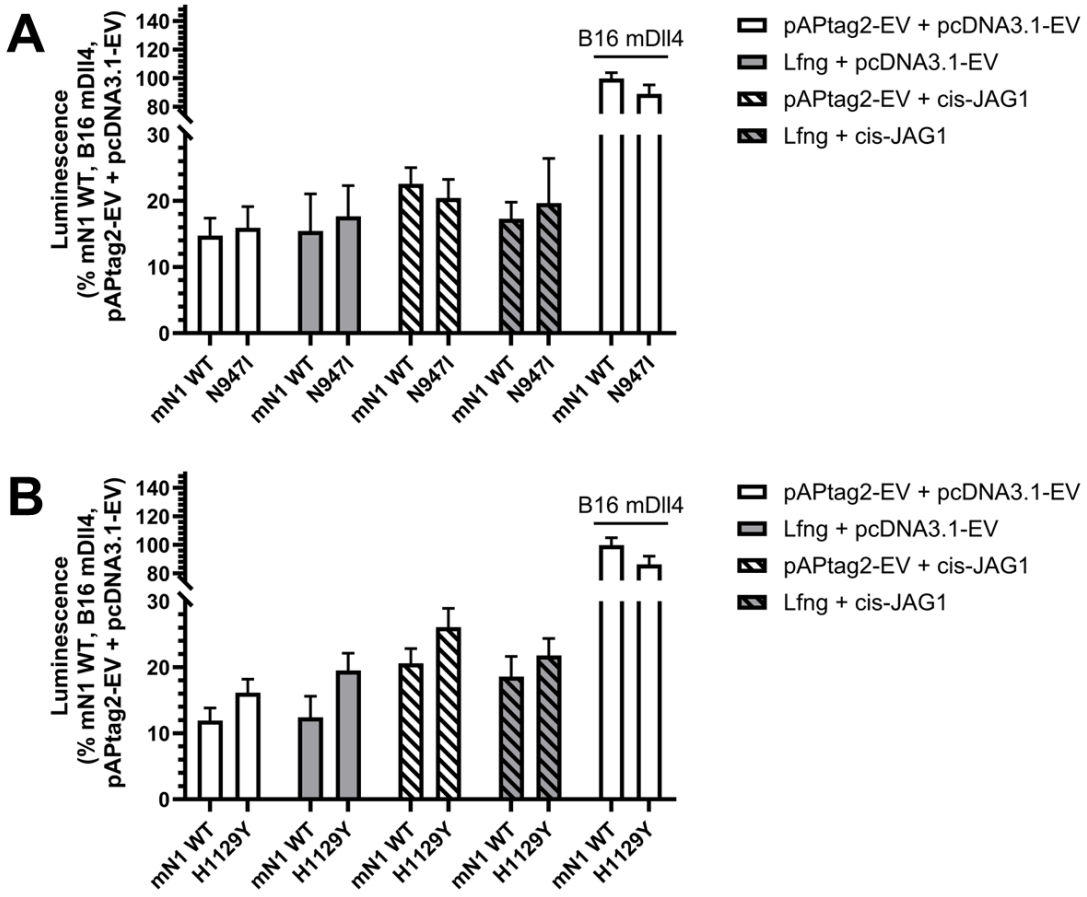

Figure G.1. Auto-activation levels of mN1 cells transfected with cis-JAG1 and Lfng.

Activation assays for mN1 WT and (A) N947I or (B) H1129Y cell lines transfected with pcDNA3.1-EV or cis-JAG1 and pAPtag2-EV or Lfng. Cells were grown with B16 WT control cells or B16 mDll4 cells. Graphs show the combined results of five independent plates, each with four repeat wells. Data presented as mean ± SD.

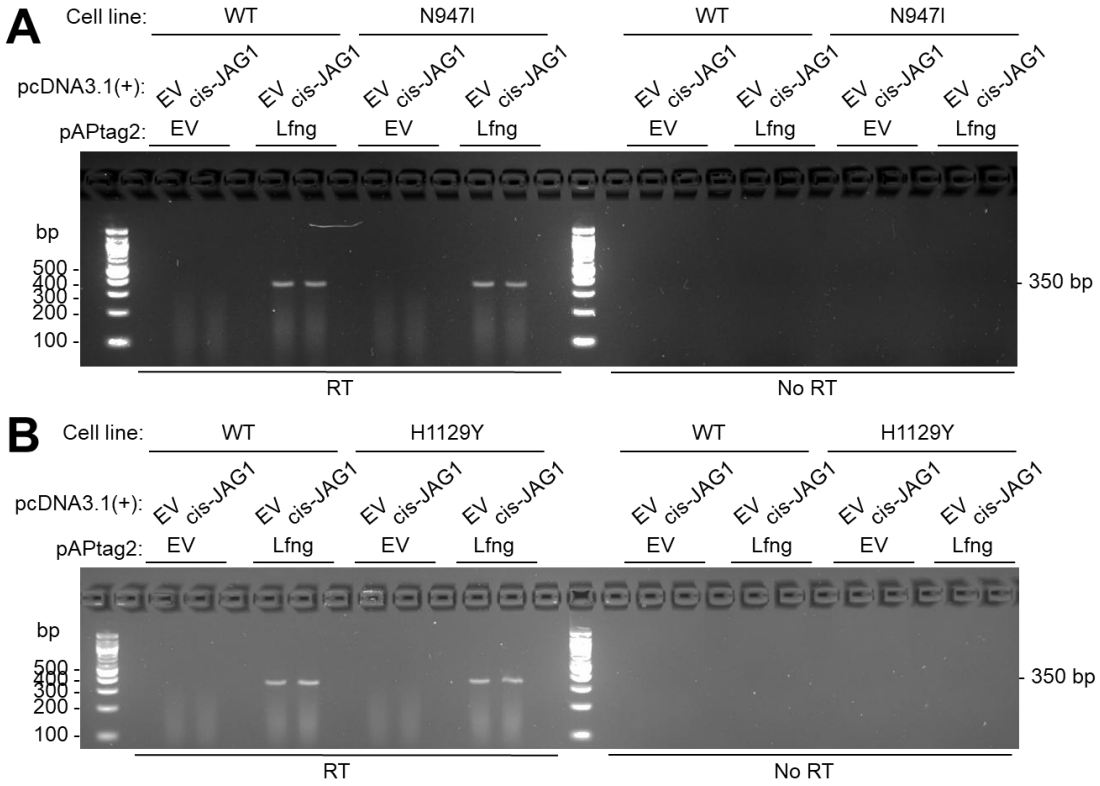

Figure G.2. RT-PCR for *Lfng* expressed in mN1 cells transfected with Lfng plasmid.

RNA was extracted from HEK-RBP mN1 WT and (A) N947I or (B) H1129Y cells co-transfected with pcDNA3.1(+) plasmid encoding JAG1 or EV and pAPtag2 plasmid encoding Lfng or EV (indicated by labels). PCRs to amplify a 350 bp region in *Lfng* cDNA were performed for RNA samples with and without RT (indicated by labels). PCR products were run on a 2.5% agarose TBE gel. For cells transfected with Lfng, RT-PCRs for *Lfng* RNA produced bands of 350 bp with equivalent intensity, suggesting comparable *Lfng* RNA expression levels.

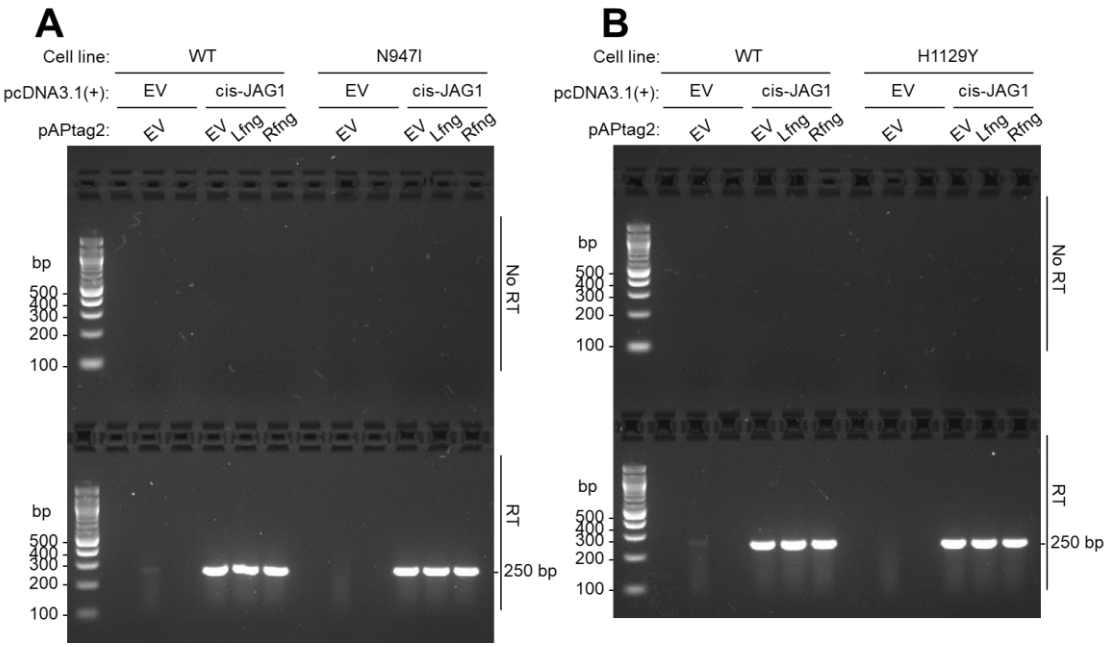

Figure G.3. RT-PCR for *JAG1* expressed in mN1 cells transfected with cis-JAG1 plasmid and Fng.

RNA was extracted from HEK-RBP mN1 WT and (A) N947I or (B) H1129Y cells co-transfected with pcDNA3.1(+) plasmid encoding JAG1 or EV and pAPtag2 plasmid encoding Lfng/Rfng or EV (indicated by labels). PCRs to amplify a 250 bp region in *JAG1* cDNA were performed for RNA samples with and without RT (indicated by labels). PCR products were run on a 2.5% agarose TBE gel. For cells transfected with cis-JAG1, RT-PCRs for *JAG1* RNA produced bands of 250 bp with equivalent intensity, suggesting comparable *JAG1* RNA expression levels. The transfection of Fng-encoding plasmids did not affect the RNA expression of *JAG1*, and vice versa.

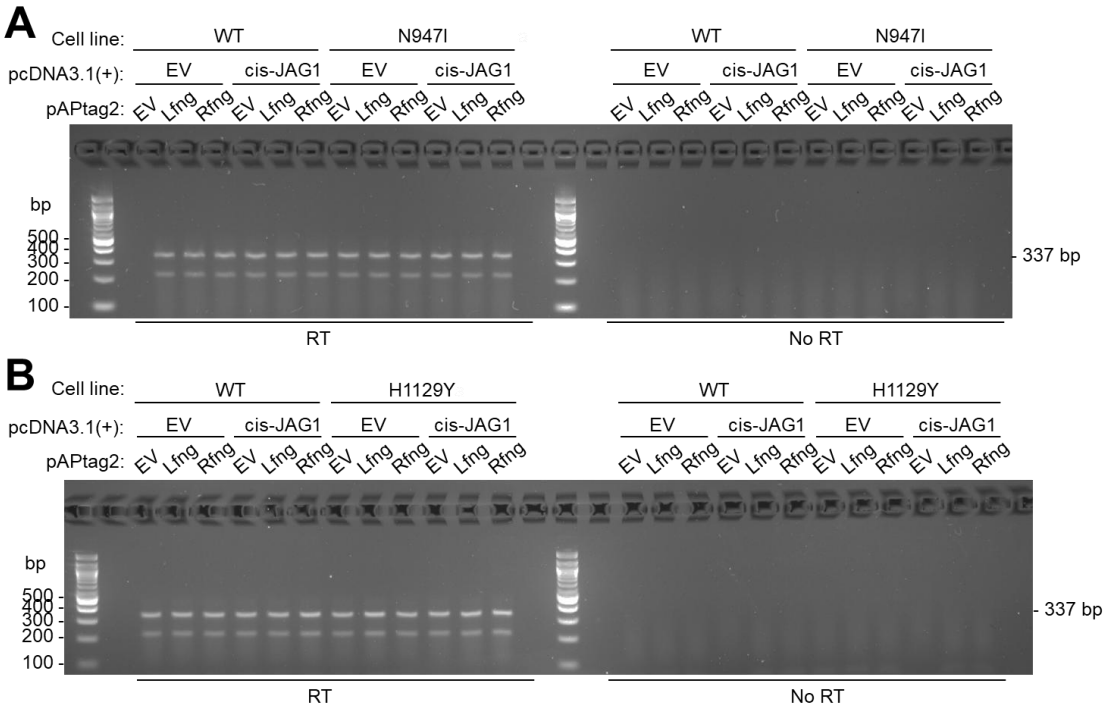

Figure G.4. RT-PCR for m*N1* expressed in mN1 cells transfected with cis-JAG1 and Fng.

RNA was extracted from HEK-RBP mN1 WT and (A) N947I or (B) H1129Y cells co-transfected with pcDNA3.1(+) plasmids encoding JAG1 or EV and pAPtag2 plasmids encoding Lfng/Rfng or EV (indicated by labels). PCRs to amplify a 337 bp region in *mN1* cDNA were performed for RNA samples with and without RT (indicated by labels). PCR products were run on a 2.5% agarose TBE gel. The band of 337 bp showed similar intensity in each sample, irrespective of whether or not Fng- or cis-JAG1-encoding plasmid was transfected. This showed that transient transfection of Fng or cis-JAG1 did not affect the stable expression of *mN1*.

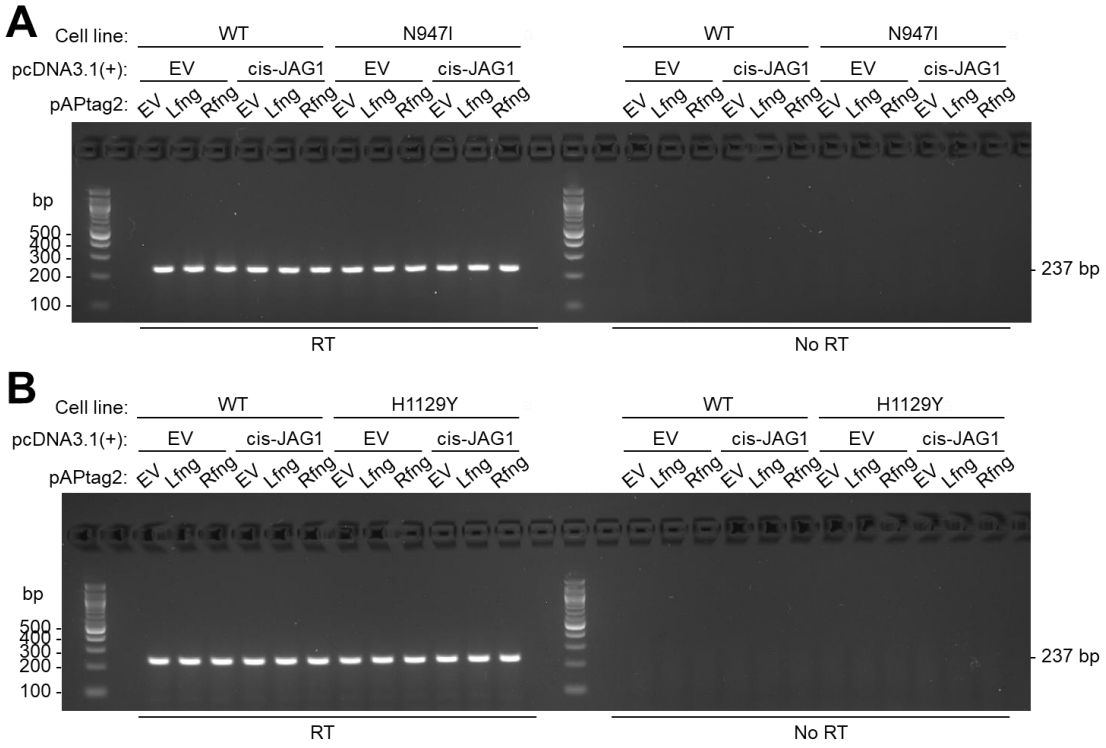

Figure G.5. RT-PCR for *GAPDH* expressed in mN1 cells transfected with cis-JAG1 and Fng.

RNA was extracted from HEK-RBP mN1 WT and (A) N947I or (B) H1129Y cells co-transfected with pcDNA3.1(+) plasmid encoding JAG1 or EV and pAPtag2 plasmid encoding Lfng/Rfng or EV (indicated by labels). PCRs to amplify a 237 bp region in *GAPDH* cDNA were performed for RNA samples with and without RT (indicated by labels). PCR products were run on a 2.5% agarose TBE gel. The band of 237 bp showed similar intensity in each sample, showing that the same starting concentration of RNA was used for RT.

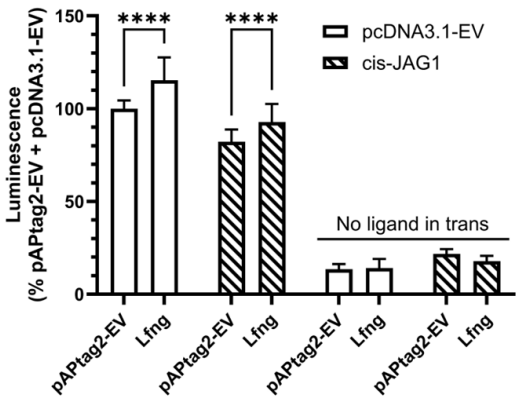

Plasmid	Luminescence (% pAPtag2-EV + pcDNA3.1-EV)	
	pcDNA3.1-EV	cis-JAG1
pAPtag2-EV	100 ± 4.457	82.18 ± 6.577
Lfng	115.3 ± 12.3	92.76 ± 9.79

Figure G.6. Dll4-mediated trans-activation of mN1 WT cells transfected with cis-JAG1 and Lfng plasmids.

Jag1-mediated cis-inhibition assays for mN1 WT cells transfected with pcDNA3.1-EV or cis-JAG1 and pAPtag2-EV or Lfng. Cells were grown with B16 mDll4 cells or B16 WT control cells (indicated by “No ligand in trans”). Graph (left panel) and table (right panel) show the combined results of at least four independent plates, each with four repeat wells. Luminescence signal in each case is shown relative to mN1 WT cells transfected with pcDNA3.1-EV and pAPtag2-EV. Data presented as mean ± SD. Statistical significance was determined by ordinary two-way ANOVA and Šídák’s post hoc test (**** = P < 0.0001).

Appendix H – SAXS

Table H.1. Peptide sequences of S2 hN1 constructs.

Construct	Peptide sequence
hN1 EGF20-27-BirA-His	NNNECESNPCVNGGTCKDMTSGYVCTCREGFSGPNCQTNINEC ASNPCLNQGTCIDDVAGYKCNCLLPYTGATCEVVLAPCAPSPCR NGGECRQSEDYESFSCVCPTGWQGQTCEVDINECVLSPCRHGA SCQNTHGGYRCHCQAGYSGRNCETDIDDCRPNPCHNGGSCTD GINTAFCDCLPGFRGTFCEEDINECASDPCRNGANCTDCVDSYT CTCPAGFSGIHCENNTPDCTESSCFNGGTCVDGINSFTCLCPPG FTGSYCQHDVNECDSQPCLHGGTCQDGCGSYRCTCPQGYTGP NCQNGSGLEVLFQGPGSLHHILDAQKMVWNHRGHHHHHHHH
hN1 EGF20-27	NNNECESNPCVNGGTCKDMTSGYVCTCREGFSGPNCQTNINEC ASNPCLNQGTCIDDVAGYKCNCLLPYTGATCEVVLAPCAPSPCR NGGECRQSEDYESFSCVCPTGWQGQTCEVDINECVLSPCRHGA SCQNTHGGYRCHCQAGYSGRNCETDIDDCRPNPCHNGGSCTD GINTAFCDCLPGFRGTFCEEDINECASDPCRNGANCTDCVDSYT CTCPAGFSGIHCENNTPDCTESSCFNGGTCVDGINSFTCLCPPG FTGSYCQHDVNECDSQPCLHGGTCQDGCGSYRCTCPQGYTGP NCQNGSGLEVLFQ
hN1 EGF20-29-BirA-His	NNNECESNPCVNGGTCKDMTSGYVCTCREGFSGPNCQTNINEC ASNPCLNQGTCIDDVAGYKCNCLLPYTGATCEVVLAPCAPSPCR NGGECRQSEDYESFSCVCPTGWQGQTCEVDINECVLSPCRHGA SCQNTHGGYRCHCQAGYSGRNCETDIDDCRPNPCHNGGSCTD GINTAFCDCLPGFRGTFCEEDINECASDPCRNGANCTDCVDSYT CTCPAGFSGIHCENNTPDCTESSCFNGGTCVDGINSFTCLCPPG FTGSYCQHDVNECDSQPCLHGGTCQDGCGSYRCTCPQGYTGP NCQNLVHWCDSSPCKNGGKCWQTHTQYRCECPSGWTGLYCDV PSVSCEVAAQRQGVDVARLCQHGGLCVDAGNTHHCRCQAGYT GSYCEDGSGLEVLFQGPGSLHHILDAQKMVWNHRGHHHHHHHH
hN1 EGF20-29	NNNECESNPCVNGGTCKDMTSGYVCTCREGFSGPNCQTNINEC ASNPCLNQGTCIDDVAGYKCNCLLPYTGATCEVVLAPCAPSPCR NGGECRQSEDYESFSCVCPTGWQGQTCEVDINECVLSPCRHGA SCQNTHGGYRCHCQAGYSGRNCETDIDDCRPNPCHNGGSCTD GINTAFCDCLPGFRGTFCEEDINECASDPCRNGANCTDCVDSYT CTCPAGFSGIHCENNTPDCTESSCFNGGTCVDGINSFTCLCPPG FTGSYCQHDVNECDSQPCLHGGTCQDGCGSYRCTCPQGYTGP NCQNLVHWCDSSPCKNGGKCWQTHTQYRCECPSGWTGLYCDV PSVSCEVAAQRQGVDVARLCQHGGLCVDAGNTHHCRCQAGYT GSYCEDGSGLEVLFQ

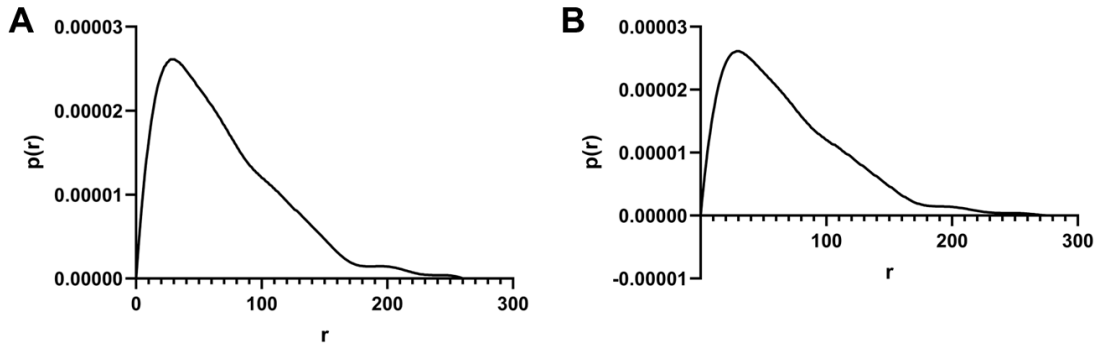

Figure H.1. P(r) distribution derived from the scattering data collected from hN1 EGF20-29.

P(r) distribution curves derived from the scattering data collected from hN1 EGF20-29 using D_{max} of (A) 260 Å and (B) 280 Å. When D_{max} was set as 280 Å, P(r) became negative (<0) when r was 279.

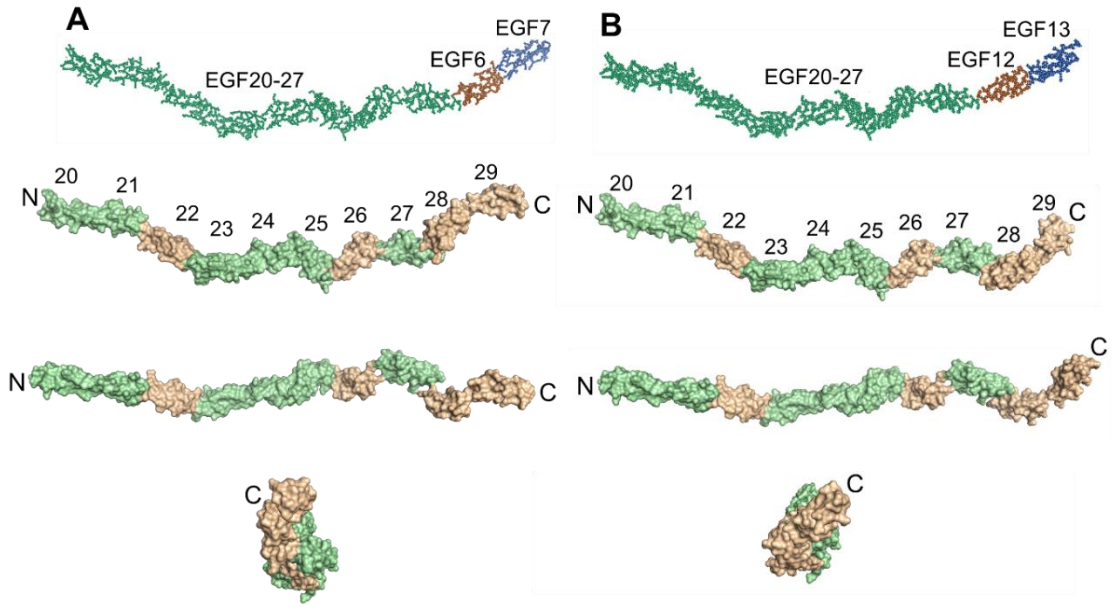

Figure H.2. Alternative models of hN1 EGF20-29 generated by SREFLEX.

(A) (Upper panel) Initial model of hN1 EGF20-29 formed by the SREFLEX-generated structure of EGF20-27 (green), EGF6 (PDB: 5FMA) for EGF28 (red) and EGF7 (PDB: 5FMA) for EGF29 (blue). (Lower panel) Optimised model (χ^2 = 5.98) of hN1 EGF20-29 generated by SREFLEX based on the initial model. The model is shown from 3 different angles. (B) (Upper panel) Initial model of hN1 EGF20-29 formed by the SREFLEX-generated structure of EGF20-27 (green), EGF12 (PDB: 5FMA) for EGF28 (red) and EGF13 (PDB: 5FMA) for EGF29 (blue). (Lower panel) Optimised model (χ^2 = 6.09) of hN1 EGF20-29 generated by SREFLEX based on the initial model. The model is shown from 3 different angles. In the lower panels, non-Ca^{2+}-binding EGF domains are shown in wheat and cbEGF domains are shown in green.

Appendix I – Discussion

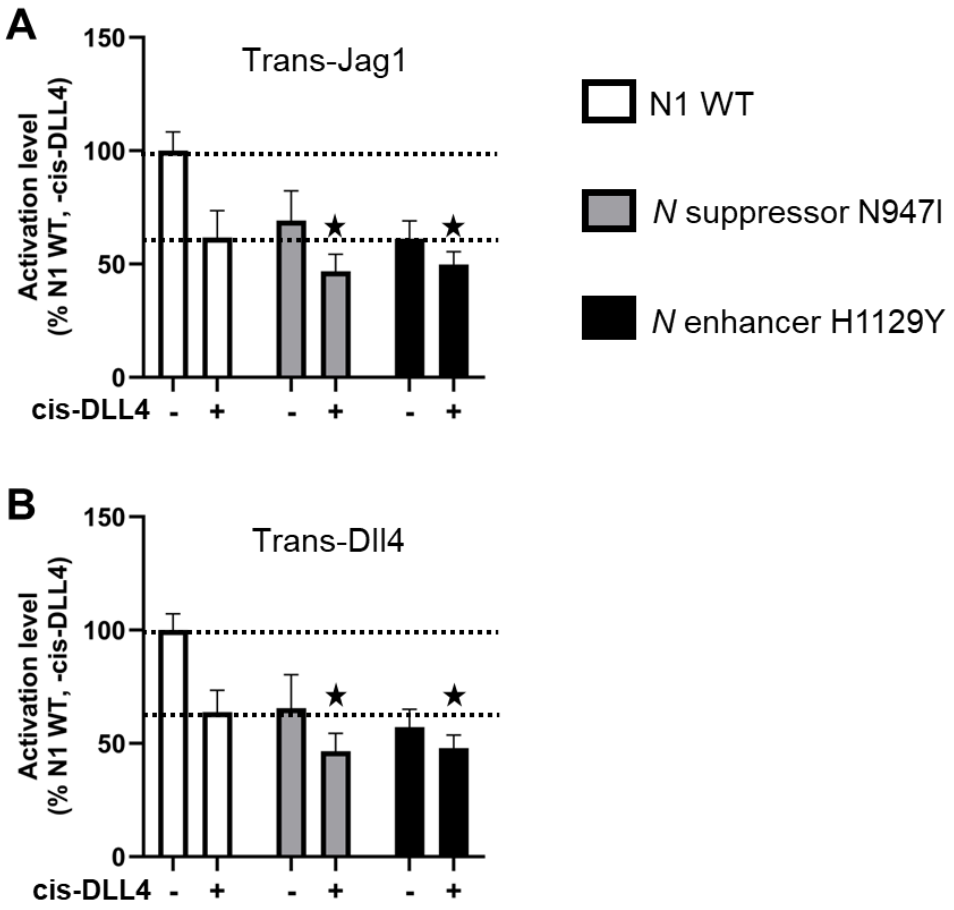

Figure I.1. Activation of N1 WT and Ax variants by different trans-ligands under conditions with and without cis-DLL4.

Activation levels of N1 WT, *N* suppressor N947I and *N* enhancer H1129Y in the absence ("-") and presence ("+") of cis-DLL4. Cells were grown with (A) trans-Jag1 or (B) trans-Dll4. Signals are shown relative to N1 WT in the absence of cis-DLL4. Data were presented as mean ± SD (extracted from Figure 5.4 and 5.5). Activation levels of Ax variants that are statistically different to that of N1 WT in the presence of cis-DLL4 are indicated by stars.